APPLIED ORGANOMETALLIC CHEMISTRY
Appl. Organometal. Chem. 2004; **18**: 227–232
Published online in Wiley InterScience (www.interscience.wiley.com). DOI:10.1002/aoc.612

High-resolution ^{15}N solid-state NMR investigations on borazine-based precursors

Bérangère Toury[1], Christel Gervais[1]*, Philippe Dibandjo[2], David Cornu[2], Philippe Miele[2] and Florence Babonneau[1]

[1]Laboratoire de Chimie de la Matière Condensée, UMR CNRS 7574, Université Pierre et Marie Curie, 4 place Jussieu, Tour 54, Etage 5, 75252 Paris Cedex 05, France
[2]Laboratoire des Multimatériaux et Interfaces, UMR CNRS 5615, Université Claude Bernard Lyon 1, 43 bd du 11 novembre 1918, 69622 Villeurbanne Cedex, France

Received 15 December 2003; Revised 31 December 2003; Accepted 9 January 2004

Reference compounds based on borazine units and polyborylborazines have been characterized by ^{15}N solid-state NMR. The various nitrogen sites (B_3N, B_2NH, B_2NX (X = H, Me, ^iPr), BN(H)X and BNX_2 (X = Me, ^iPr) have been discriminated according to their cross-polarization behaviour and chemical shift values, which range from −265 to −350 ppm. This has permitted the elucidation of the polymerization mechanism associated with the polycondensation of two borazine-based derivatives. In particular, this technique appears to be a powerful investigation tool for finding whether the B_3N_3 rings are linked through three-atom N–B–N aminoboryl bridges or connected by direct B–N bonds.

KEYWORDS: borazine; polymerization mechanism; ^{15}N CP-MAS NMR

INTRODUCTION

Boron nitride is an artificial, important non-oxide ceramic exhibiting a combination of particular attractive properties,[1] including low density, high temperature stability and strength, low dielectric constant and thermal conductivity and high-temperature oxidation resistance. Therefore, is suitable for a wide range of applications, particularly in the field of high-temperature structural materials. The use of high-performance hexagonal boron nitride (h-BN) fibres as a toughening agent is attractive in the fabrication of ceramic-matrix composites and metal-matrix composites.[2] Pre-ceramic precursor pyrolysis has been shown to be the most promising route for producing fibres.[3] This process consists of the synthesis of a molecular precursor, its polymerization into a melt-spinnable polymer, and finally the conversion of the shaped crude article into h-BN fibres.[4] The influence of the polymer architecture on the structure of the final ceramic has been clearly demonstrated for Si–C[5] and Si–C–N[6] systems. Likewise, recent studies performed on the synthesis of BN fibres from borazinic derivatives have shown a close relationship between the polymeric precursor structure, its processing properties and the performances of the derived BN fibres.[7,8] Therefore, it appears essential to control as much as possible the polymerization and the ceramization steps to improve the material properties. This control requires suitable characterization tools to follow the monomer-to-polymer and polymer-to-ceramic conversions. The aim of this study is to show how the ^{15}N solid-state NMR technique can be extremely useful and relevant in understanding the polymerization mechanisms and the ceramization processes.

^{15}N is a $\frac{1}{2}$ spin nucleus with a very low sensitivity in natural abundance (3.8×10^{-6} compared with ^1H), but this drawback may be overcome by using cross-polarization (CP) techniques, taking advantage of the ^1H–^{15}N dipolar coupling. This method is consequently very sensitive to the proton environment of the nitrogen sites through the ^1H–^{15}N distances and the molecular motion. Recent studies on B–N containing reference compounds and borazine-derived polymers have shown that it is possible to distinguish nitrogen sites depending on their degree of protonation by using the inversion recovery CP (IRCP) sequence.[9,10]

Until now, the most promising results concerning BN fibres were obtained with borazine-based precursors.[7,8,11–15] This paper reports the findings of a preliminary study

*Correspondence to: Christel Gervais, Laboratoire de Chimie de la Matière Condensée, UMR CNRS 7574, Université Pierre et Marie Curie, 4 place Jussieu, Tour 54, Etage 5, 75252 Paris Cedex 05, France.
E-mail: gervais@ccr.jussieu.fr

carried out on five borazinic compounds (monomers) and two polyborazines (polymers). In order to define the ^{15}N chemical shift ranges for different nitrogen environments, compounds 2,4,6-$(CH_3HN)_3B_3N_3H_3$ (**I**), 2,4,6-$[(CH_3)_2N]_3B_3N_3H_3$ (**II**), 2,4,6-$\{[(CH_3)_2CH]_2N\}_3B_3N_3H_3$ (**III**), 2,4,6-$\{[(CH_3)_2CH]N(H)\}_3B_3N_3H_3$ (**IV**) and 2,4,6-$\{[(((CH_3)_2CH)_2N)_2B]N(CH_3)\}$ (**V**) were synthesized and analysed. Two polymers prepared from borylborazines were then investigated to elucidate the polymerization mechanisms and the resulting polymer structures.

EXPERIMENTAL

Sample preparation

All experiments were performed under argon atmosphere and anhydrous conditions using standard vacuum-line, Schlenk techniques and an efficient dry-box with solvents purified by standard methods.

*Synthesis of tri(monoalkylamino)borazine (**I** and **IV**) and tri(dialkylamino)borazine (**II** and **III**)*

Compounds **I**, **II**, **III** and **IV** were prepared using a previously described procedure[16,17] with slight modifications. 2,4,6-Trichloroborazine ($Cl_3B_3N_3H_3$)[18] (~2 g, 10.9 mmol) was dissolved in toluene (40 ml) and excess (8 : 1) of the appropriate amine (methylamine, dimethylamine, diisopropylamine and isopropylamine for **I**, **II**, **III** and **IV** respectively) was added to the solution at −20 °C. The mixture was allowed to warm up to room temperature under stirring (24 h). The resulting solution was filtered under argon. The residue was washed with toluene (20 ml) and the combined filtrate and extract solutions were evaporated to yield a powder.

*Synthesis of 2,4,6-tri[bi(diisopropylamino)boryl-(methylamino)]borazine (**V**)*

In a typical experiment, a solution of $(MeHN)B(N^iPr_2)_2$ (3.62 g, 15.0 mmol) in toluene (50 ml) was added slowly at −20 °C to a solution of $Cl_3B_3N_3H_3$ (0.92 g, 5.0 mmol) and Et_3N (5 g) in toluene (100 ml).[19] The mixture was stirred for 2 h at room temperature. The residue was filtered off and the filtrate was evaporated, yielding a white powder. By recrystallization in hexane, the product yields a crystalline solid **V**. Yield 99.5% (trichloroborazine).

*Preparation of polymers **VI** and **VII***

Polymers were prepared by different processing routes.

Polymer **VI**: 2,4-di(chloro)-6-(dimethylamino)borazine ($Cl_2[(CH_3)_2N]B_3N_3H_3$; 4.6 g, 24.2 mmol) in toluene (100 ml) were slowly added at −10 °C under stirring to a solution of tri(methylamino)borane ($B(NHCH_3)_3$; 2.6 g, 24.2 mmol) and Et_3N (15 ml). After the addition, the mixture was stirred for a further 1 h at −10 °C and then for 24 h at room temperature. The residue was filtered off and the filtrate was evaporated, yielding a yellow powder. To compact the product, the powder was heated at 150 °C for 15 min. Polymer **VI** (5.2 g) was collected as a yellow granular solid.

Polymer **VII**: 9.9 g (15.7 mmol) of $[(NH^iPr)_2B(N^iPr)]_3B_3N_3H_3$ were heated *in vacuo* (10^{-4} mmHg) at 70 °C for 2 h, 90 °C for 1 h, 100 °C for 1.5 h, 120 °C for 2.25 h, 140 °C for 30 min, and finally at 150 °C for 1.5 h. Polymer **VII** was collected (5.8 g) as a yellow granular solid.

NMR experiments

^{15}N CP-MAS experiments were performed at room temperature on a Bruker MSL-300 spectrometer, at frequencies of 30.41 MHz (^{15}N) and 300.13 MHz (^1H), using a Bruker CP-MAS probe. Solid samples were spun at 5 kHz, using 7 mm ZrO_2 rotors filled up in a glove-box under a dried argon atmosphere. All ^{15}N CP-MAS experiments were performed under the same Hartmann–Hahn match condition, set up by using a powdered sample of NH_4NO_3: both radio-frequency channel levels $\omega_{1H}/2\pi$ and $\omega_{15N}/2\pi$ were carefully set so that $|\omega_{1H}|/2\pi = |\omega_{15N}|/2\pi = 42$ kHz. Proton decoupling was always applied during acquisition; a repetition time of 10 s and a contact time of 2 ms were used. Chemical shifts were referenced to solid NH_4NO_3 (10% ^{15}N-enriched sample, $\delta_{iso}(^{15}NO_3) = -4.6$ ppm compared to CH_3NO_2 ($\delta = 0$ ppm)). Liquid ^{11}B NMR spectra were recorded on a Bruker DRX500 spectrometer at a frequency of 160.461 MHz with $Et_2O{\cdot}BF_3$ as an external reference in toluene solution.

RESULTS AND DISCUSSION

Previous investigations on the preparation of h-BN fibres by the pre-ceramic polymer route have clearly demonstrated the need for a tailored polymeric precursor with enhanced processing properties. Actually, according to several workers,[7,8,14,15] good melt-spinning conditions, which are presumably the crucial step in this process, can be obtained by using polymers displaying hydrocarbon chains and by controlling the nature of the linkages between the borazinic rings within the polyborazines. During the monomer-to-polymer conversion of alkylaminoborazines, different reactions[20,21] may occur: establishment of –N(R)– bridges or direct B–N bonds between two rings (Fig. 1), and ring-opening or fusion mechanisms. Logically, the polymer-processing properties will depend on its structure. For example, a polymer displaying high cross-linking or having fused-cycle segments should be infusible and consequently impossible to turn into crude fibres.[14,15] Moreover, a close relationship between the monomer structure, its behaviour under heating and the spinnability of the resulting polymer has recently been demonstrated.[7,8] In this context, it appears very interesting to understand better the exact polymer architecture and polymerization reactions to predict the polymer melt-spinning ability.

The ^{15}N chemical shift values of the different nitrogen environments extracted from the simulation of the spectra

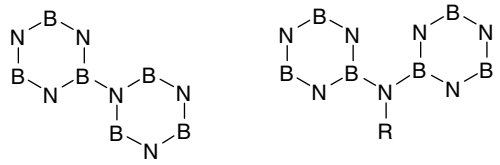

Figure 1. Different linkages observed in polyborazine obtained by thermolysis of trialkylaminoborazine.

Table 1. ^{15}N chemical shift values of the different nitrogen environments extracted from the simulation of the spectra recorded for samples **I** to **VII**

	δ (ppm)						
Assignment	**I**	**II**	**III**	**IV**	**V**	**VI**	**VII**
B_2NH	−313	−309	−310	−307	−301	−311	−310
B_3N							−286
B_2NMe					−327	−326	
B_2N^iPr							−266
$BNMe_2$		−342				−340	
BN^iPr_2			−299		−290		
BN(H)Me	−347					−348	
$BN(H)^iPr$				−293			−287

recorded for the compounds and polymers discussed below are summarized in Table 1.

Monomers

Two pairs of borazines were chosen as reference compounds: tri(methylamino)borazine (**I**) and tri(dimethylamino)-borazine (**II**), and tri(diisopropylamino)borazine (**III**) and tri(isopropylamino)borazine (**IV**). Each compound displays two nitrogen sites with different environments: B_2NH and BNRR′ with R = H, R′ = Me (**I**), R = R′ = Me (**II**), R = R′ = ^{i}Pr (**III**) and R = H, R′ = ^{i}Pr (**VI**). Another monomer was chosen as reference: the tri[bi(diisopropylamino)boryl(methylamino)]borazine (**V**), a borylborazine (B_3N_3 ring linked to three aminoboryl groups) showing three different nitrogen sites: B_2NH, B_2NMe and BN^iPr_2. Compounds **I** to **V** are shown in Fig. 2.

The ^{15}N CP-MAS spectra of these five samples (Fig. 3) show signals ranging from −280 to −350 ppm, with peaks appearing at higher field for samples **I**, **II** and **V** containing N–Me bonds. The IRCP sequence[22–25] was used in order to distinguish the nitrogen sites according to their degree of protonation and differentiate NH groups from non-protonated nitrogen groups in samples **II**, **III** and **V**. The signals of protonated nitrogen sites, which present a more intense ^{15}N–^1H dipolar coupling, are indeed expected to invert (with increasing inversion time) more rapidly than non-protonated nitrogen atoms showing longer inversion time values.[9]

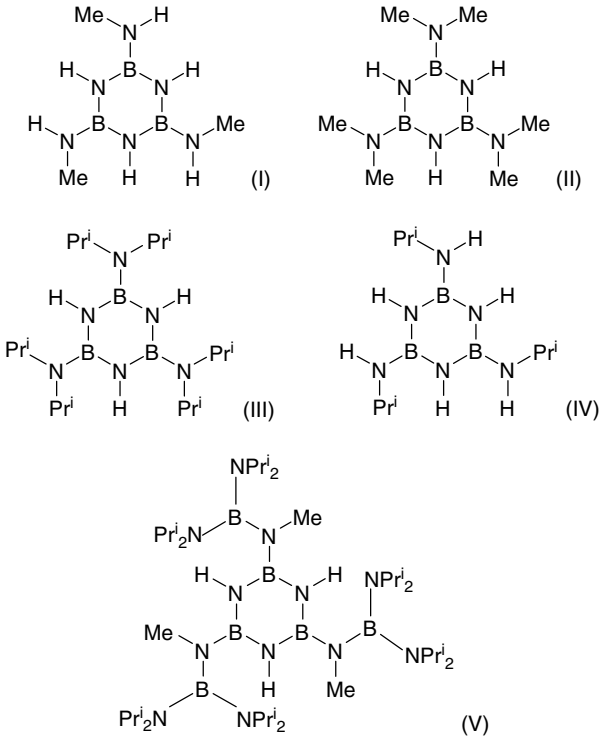

Figure 2. Schematic representations of tri(monomethylamino)-borazine (**I**), tri(dimethylamino)borazine (**II**), tri(diisopropylamino)-borazine (**III**), tri(monoisopropylamino)borazine (**IV**) and tri[bis-(diisopropylamino)boryl(methylamino)]borazine (**V**).

Compound II

Two signals are clearly resolved at −309 and −342 ppm in the ^{15}N IRCP MAS spectra (Fig. 4), in good agreement with the presence of two nitrogen sites in the proposed structure of this compound (Fig. 2). The first peak (−309 ppm), inverting more rapidly, can be assigned to a B_2NH environment, and the second probably corresponds to the $BNMe_2$ site.

Compound III

Two narrow signals are observed at −299 ppm and −310 ppm. The first one inverts at a slower rate (Fig. 4), which suggests that they can be assigned to BN^iPr_2 and B_2NH environments respectively.

Compound V

Three different sites are expected in this sample (Fig. 2), which is not obvious on the ^{15}N CP-MAS spectrum (Fig. 3). This shows two main signals, centred at −305 and −327 ppm. The ^{15}N IRCP-MAS spectra (Fig. 4) show the presence of two components in the peak at lower field. The one at −290 ppm inverts at a slowes rate than the one at −301 ppm, which exhibits an IRCP behaviour characteristic of an NH environment and therefore, is assigned to B_2NH. The signal at −290 ppm can be attributed to BN^iPr_2, in good agreement with the previous results obtained on sample **III**; the last signal, at −327 ppm, corresponds to B_2NMe boryl bridges.

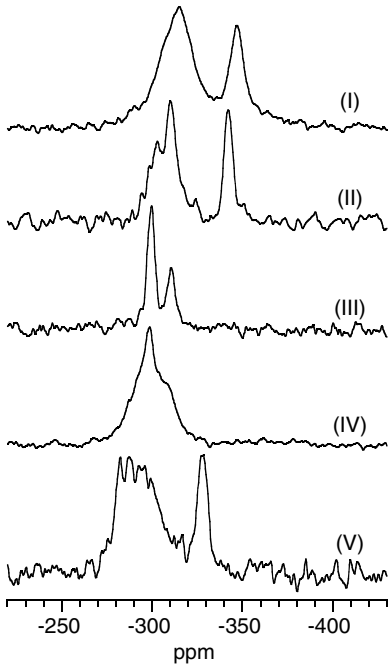

Figure 3. ^{15}N CP-MAS NMR spectra of compounds **I**, **II**, **III**, **IV** and **V**.

Compounds I and IV

As shown in Fig. 3, two signals showing similar IRCP behaviour characteristic of NH groups are found at −313 and −347 ppm in sample **I** and at −293 and −307 ppm in sample **IV**. By comparison with the results obtained for the other compounds showing B_2NH signals between −301 and −310 ppm, the peaks at −307 and −313 ppm were assigned to B_2NH environments. Regarding the structures of these two compounds (Fig. 2), the signals at −347 ppm and −293 ppm were then attributed to BN(H)Me and BN(H)^{i}Pr sites respectively.

Polymers

Polymers **VI** and **VII** were prepared using two synthesis routes in order to observe different polymer structures due to different polymerization mechanisms. Actually, polymer **VI**, obtained at room temperature, should display only one kind of inter-cyclic bond, a three-atom bridge due to the elimination of one chlorine atom from the borazine derivative and one hydrogen atom from the aminoborane (Fig. 5). Moreover, every borazinic ring holds a dimethylamino group. Polymer **VII** should present a different structure, since the thermolysis of $[(NH^iPr)_2B(N^iPr)]_3B_3N_3H_3$ can be considered through two possible condensation mechanisms,[26] the formation of direct B–N bonds between the rings or their linkage through amino bridges (Fig. 6). From previous results,[26] the second mechanism is expected to be predominant because of the steric hindrance of the highly encumbered $-N(^iPr)B(NH^iPr)_2$ groups.

The ^{15}N CP-MAS spectra of polymers **VI** and **VII** show composite signals of overlapping peaks ranging from −280 to −360 ppm and from −250 to −320 ppm respectively (Fig. 7). It can be noticed that the signals of polymer **VI** (containing N–Me bonds) appear at higher field than those of the polymer **VII** (containing N–^{i}Pr bonds), in good agreement with the results described above on the reference borazines **I** to **V**.

A series of IRCP experiments spectra were recorded on each sample to show the different components of these signals, taking advantage of their different inversion rates. All the spectra recorded for various inversion times were simulated with a single set of peaks by keeping the chemical shift values, line widths and shapes constant and by fitting only the peak amplitudes for each spectra.

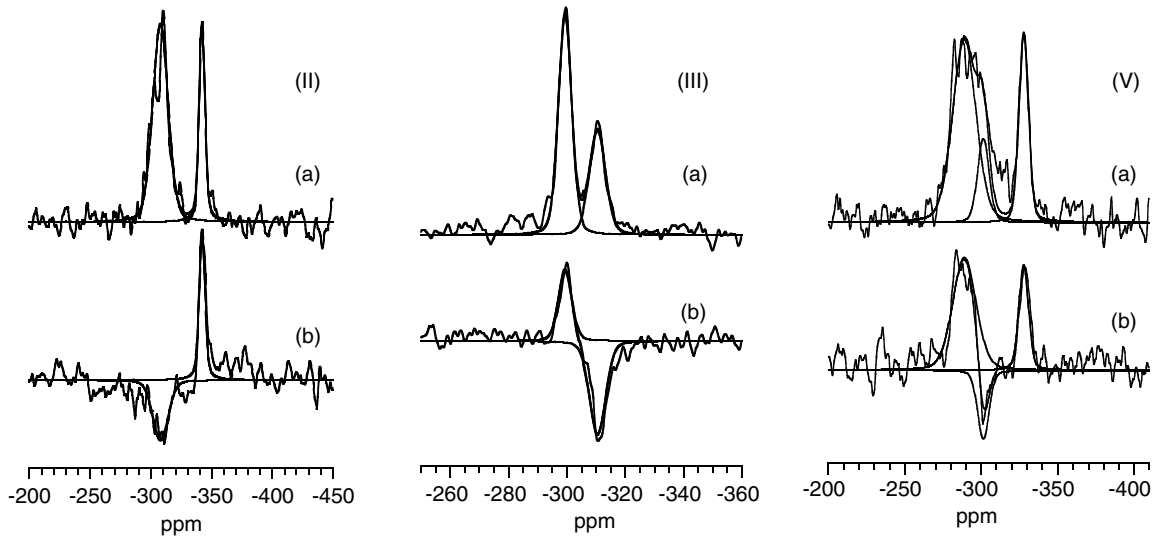

Figure 4. ^{15}N IRCP-MAS NMR spectra of compounds **II**, **III** and **V** at two inversion time values: (a) 5 μs; (b) 125 μs.

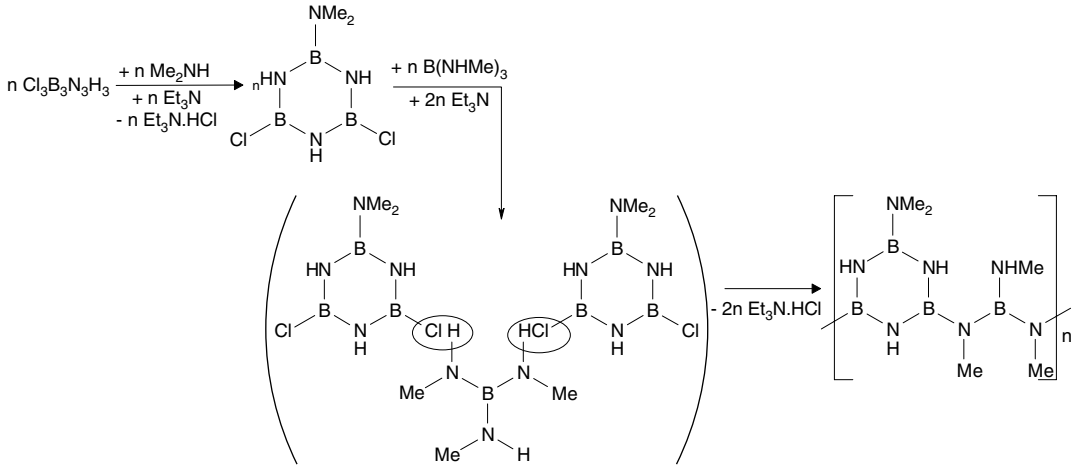

Figure 5. Condensation reactions leading to polymer **VI**.

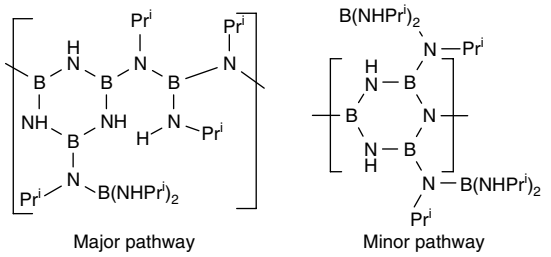

Figure 6. Different linkages observed in polymer **VII**.

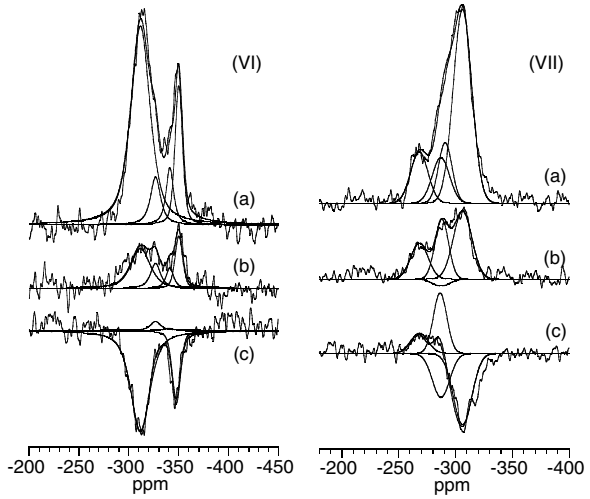

Figure 7. ^{15}N IRCP-MAS NMR spectra of polymers **VI** and **VII** at three inversion time values: (a) 5 μs; (b) 125 μs; (c) 500 μs.

*Polymer **VI***

Four peaks were necessary to reproduce the shape of the spectra for each inversion time (Fig. 7). Two peaks at −311 ppm and −348 ppm exhibit an IRCP behaviour characteristic of NH environments and can be assigned to B_2NH and BN(H)Me sites respectively, in good agreement with the corresponding chemical shift values observed in sample **I**. Two peaks at −326 ppm and −340 ppm invert at a much slower rate and can, therefore, be assigned to non-protonated nitrogen groups (B_2NMe and $BNMe_2$ respectively) according to the position of these peaks in samples **II** and **V** and in good agreement with the proposed structure of this polymer (Fig. 5). These assignments, and more particularly the presence of B_2NMe boryl bridges, were confirmed by the corresponding ^{11}B liquid-state NMR spectrum showing four peaks at 24.7, 26.0, 27.7 and 31.2 ppm. The last two signals can be assigned to borazinic BN_3 environments[10,27] and the peak at 24.7 ppm corresponds to terminal aminoboryl groups. This is in good agreement with the ^{11}B NMR spectrum of $[(Me(H)N)_2B(Me)N]_3B_3N_3H_3$, which shows a signal at 23.4 ppm.[27] The peak appearing at 26.0 ppm can, therefore, be attributed to the bridging aminoboryl groups.[27]

*Polymer **VII***

Four peaks were also extracted from the simulation of the different IRCP spectra (Fig. 7). Two of them, at −287 ppm and −310 ppm, invert rapidly and can be assigned to $BN(H)^iPr$ and B_2NH environments respectively, according to the results for borazine **IV**. A peak at −286 ppm with an IRCP behaviour characteristic of a non-protonated nitrogen can be tentatively assigned to a B_3N environment, since its position is close to that observed in h-BN.[10] This confirms that some of the borazine rings are directly connected through B–N bonds. Finally, a signal corresponding to a tertiary nitrogen is observed at −266 ppm and probably corresponds to a B_2N^iPr site according to the proposed structure of this polymer (Fig. 6). This is also in good agreement with an observed shift at lower field of almost 50 ppm between BNX_2 or BN(H)X sites for X = ^{i}Pr compared with X = Me (Table 1). Since the ^{15}N chemical shift value of B_2NMe has been measured at around −326 ppm in sample **III** and **VI**, the chemical shift value of B_2N^iPr is effectively expected around −266 ppm.

^{15}N CP-MAS experiments are not quantitative and, therefore, it is difficult to estimate the relative proportion of B_3N and B_2N^iPr environments in polymer **VII**.

CONCLUSIONS

This study has shown the relevance of ^{15}N CP-MAS NMR experiments in discriminating B_3N, B_2NH, B_2NX ($X = H$, Me, ^{i}Pr), BN(H)X and BNX_2 ($X = Me$, ^{i}Pr) environments according to their chemical shift values, which range from −265 to −350 ppm. It is worth noting that the nature of the alkyl group induces a shift of almost +50 ppm in going from a methyl to isopropyl group.

Therefore, it is possible with this technique to distinguish borazinic from aminoboryl environments, and this permitted the elucidation of the polymerization mechanism associated with the polycondensation of two borazine-based derivatives. The condensation at room temperature of a chloroborazine with an aminoborane as intermediate leads to a polymer displaying only aminoboryl bridges between the rings. In the case of the thermolysis of a borylboraine, the B_3N_3 rings appear to be linked through three-atom N–B–N boryl bridges, but they are also connected by direct B–N bonds. The next step in this study will be to understand better the influence of the structure of the polymers on their melt-spinnability behaviour.

REFERENCES

1. Paine RT, Narula CK. *Chem. Rev.* 1990; **90**: 73.
2. Rice RW. *Am. Ceram. Soc. Bull.* 1983; **62**: 889.
3. Wynne KJ, Rice R. *Annu. Rev. Mater. Sci.* 1984; **14**: 297.
4. Paine RT, Sneddon LG. *Chemtech* 1994; **7**: 29.
5. Laine RM, Babonneau F, Mackenzie JD. *J. Mater. Sci.* 1990; **25**: 3886.
6. Birot M, Pillot JP, Dunogues J. *Chem. Rev.* 1995; **95**: 1443.
7. Toury B, Miele P, Cornu D, Vincent H, Bouix J. *Adv. Funct. Mater.* 2002; **12**: 228.
8. Rousseau L, Pasquet JC, Bernard S, Bonnetot B, Cornu D, Favre R, Miele P, Toury B, Toutois P. *French Patent* 0 003 380, 2000.
9. Gervais C, Babonneau F, Maquet J, Bonhomme C, Massiot D, Framery E, Vaultier M. *Magn. Reson. Chem.* 1998; **36**: 407.
10. Gervais C, Maquet J, Babonneau F, Duriez C, Framery E, Vaultier M, Florian P, Massiot D. *Chem. Mater.* 2001; **13**: 1700.
11. Kimura Y. *US Patent* 5 061 469, 1991.
12. Kimura Y, Kubo Y, Hayashi N. *J. Inorg. Organometal. Polym.* 1992; **2**: 231.
13. Kimura Y, Kubo Y, Hayashi N. *Compos. Sci. Technol.* 1994; **51**: 173.
14. Wideman T, Fazen PJ, Su K, Remsem EE, Zank GA, Sneddon LG. *Appl. Organometal. Chem.* 1998; **12**: 681.
15. Wideman T, Sneddon LG. *Chem. Mater.* 1996; **8**: 3.
16. Gerrard W, Hudson HR, Mooney EF. *J. Chem. Soc.* 1962; 113.
17. Toury B, Miele P, Cornu D, Lecocq S, Bonnetot B. *Z. Kristallogr. New Cryst. Struct.* 2001; **216**: 115.
18. Brown CA, Laubengayer AW. *J. Am. Chem. Soc.* 1955; **77**: 3699.
19. Toury B, Cornu D, Lecocq S, Miele P. *Appl. Organometal. Chem.* 2003; **17**: 68.
20. Toeniskoetter RH, Hall FR. *Inorg. Chem.* 1963; **2**: 29.
21. Paciorek KJL, Krone-Schmidt W, Harris DH, Kratzer RH, Wynne KJ. ACS Symposium Series, No. 360. American Chemical Society: Washington, DC, 1988; 392.
22. Wu X, Zhang S, Wu X. *Phys. Rev. B* 1988; **37**: 9827.
23. Wu X, Zilm KW. *J. Magn. Reson.* 1993; **102**: 205.
24. Hirschinger J, Hervé M. *Solid State NMR*, 1994; **3**: 121.
25. Sangill R, Rastrup-Andersen N, Bildsoe H, Jakobsen HJ, Nielsen NC. *J. Magn. Reson.* 1994; **107**: 67.
26. Cornu D, Miele P, Toury B, Bonnetot B, Mongeot H, Bouix J. *J. Mater. Chem.* 1999; **9**: 2605.
27. Toury B, Duperrier S, Cornu D, Bernard S, Chassagneux F, Parola S, Miele P In *Proceedings of the 105th Annual Meeting & Exposition of the American Ceramic Society* 2003; **154**: 61.

